DOI: 10.1021/ma900600n

Macromolecules
ARTICLE

Effect of Chain Architecture on the Compatibility of Block Copolymer/Nanoparticle Blends

Jessica Listak,[†] Ilhem F. Hakem,[†] Hyung Ju Ryu,[†] Sofia Rangou,[‡] Nikolaos Politakos,[‡] Konstantinos Misichronis,[‡] Apostolos Avgeropoulos,*[,‡] and Michael R. Bockstaller*[,†]

[†]*Department of Materials Science and Engineering, Carnegie Mellon University, 5000 Forbes Ave., Pittsburgh, Pennsylvania 15213, and* [‡]*Department of Materials Science and Engineering, University Campus, University of Ioannina, Ioannina 45110, Greece*

Received March 20, 2009; Revised Manuscript Received June 27, 2009

ABSTRACT: The effect of block copolymer chain connectivity on the structure formation in binary blends comprising block copolymer hosts and enthalpically neutralized particle fillers is investigated for linear diblock (AB) and triblock (ABA and BAB) as well as four-arm star copolymer architectures (AB_3 and A_3B). For particles with approximately constant effective size (defined here as the ratio of filler particle diameter to host polymer radius of gyration), miscibility was observed only within diblock copolymers and within the domains formed by the end blocks of triblock copolymers. The limitation of particle miscibility within the triblock mid-domain is interpreted as a consequence of the entropy loss associated with particle deposition due to the stretched configuration of bridged midblock chains. Particle aggregation was observed in both star copolymer samples irrespective of the architecture of the particle-loaded polymer domain. In the case of particle loading of the branched copolymer domain, this is rationalized as a consequence of the increased effective particle size, whereas the incompatibility of particle fillers in the linear block domain of miktoarm copolymer hosts is interpreted as a result of the coupling of dimensional changes within the microstructure along with the reduced axial compressibility of the particle-free branched domain. The sensitive dependence of the particle compatibility on the chain architecture of the polymer host illustrates a yet unexplored parameter space that will need to be taken into account if particle blends are to be designed with branched or multiblock host copolymer architectures.

Introduction

The development of multiphase nanomaterials with structural control over multiple length scales and properties that capitalize on the synergy between their constituents is widely recognized to play a major role in future technology-enabling processes.[1] In this context, self-assembly processes have attracted particular interest as they provide a practical and efficient route toward complex hierarchically ordered structures with size ranges that cannot yet be viably accessed by established lithographic techniques.[2] Much effort has been directed on harnessing the self-organization of block copolymers as a platform for microstructured hybrid materials—either by coassembly of block copolymers with appropriately modified particle fillers (which is the focus of the present paper) or by in situ synthesis of particle inclusions within appropriately functionalized block copolymer templates.[3−5] Research in block copolymer/nanoparticle (BCP/NP) composites is motivated by the intriguing opportunities for engineering novel material properties that result from combining the particular electronic, optical, or magnetic characteristics of nanosized matter with the structural and mechanical properties as well as the processability of block copolymer template materials. For example, BCP/NP composites have been proposed as a material platform for applications ranging from catalysts to polymer-based photonic crystals to high-efficiency nonlinear optical materials.[6,7] Furthermore, the localization of nanoparticles within particular regions of the copolymer microstructure has been shown to provide a means for tuning material properties beyond the possibilities of homogenized polymer/particle composites.[8] In order to facilitate future impact of these material systems, research has to accomplish understanding of the governing parameters that control structure formation in BCP/NP blends.

Seminal work by Ausserré and co-workers as well as Lauter-Pasyuk et al. on polystyrene-functionalized ferrite nanocrystals co-organized with poly(styrene-*b*-methyl methacrylate) (PS−PMMA) was the first to suggest that particle segregation within the BCP domain microstructure sensibly depends on the characteristic length scales of the constituents, i.e., the particle-to-polymer domain size ratio $s = d_P/R_G$, with d_P denoting the particle diameter and R_G the radius of gyration of the particle-loaded polymer host.[9−11] Support for the relevance of s on the structure formation process in BCP/NP blends was provided by numerical simulations using a combined self-consistent field/density functional theory (SCFT/DFT) introduced by Balazs and co-workers.[12−14] In particular, enthalpically neutralized particle fillers were predicted to segregate to the domain interface or the domain center region in the limit of small ($s \ll 1$) and large ($s \cong 1$) particle diameter, respectively. Subsequent experiments by Bockstaller et al. demonstrated that particle inclusions with similar surface chemistry but different diameter can be combined in ternary BCP/NP1/NP2 blends to form hierarchically ordered multicomponent composite materials in which the different particle species assume distinct locations within a microdomain.[15] It should be noted, however, that the different segregation characteristics reported in the latter study are the consequence of a superposition of size effects as well as variations in particle−polymer interactions due to the somewhat different particle surface chemistry. Experiments by Kramer and co-workers using particle fillers with systematically varied grafting density

*Corresponding authors: e-mail aavger@cc.uoi.gr, Ph +30 26510 07316, Fax +30 26510 07034 (A.A.); e-mail bockstaller@cmu.edu, Ph ++1 412 268 2709, Fax ++1 412 268 7247 (M.R.B.).

 Published on Web 07/15/2009

and graft composition have confirmed that interfacial segregation is driven by the minimization of surface energy for particles with mutual affinity to both polymer domains.[16,17] More recent studies have been focused on the effect of filler concentration on order−order and order−disorder transitions of the polymer host as well as the effect of particle additives on the stabilization of defect structures in BCP/NP blends.[18−22] Further advancements in the development of theoretical techniques to predict structure formation in BCP/NP systems include novel analytical and computational models that more accurately account for particle−polymer interactions as well as kinetic effects.[23−26] These simulations suggest that prior conclusions about entropy-driven interfacial segregation of small particle fillers ($s \ll 1$) need to be revised and rather predict more uniform particle distribution with decreasing s.[24,25]

A common thread in all previous experimental and theoretical studies has been the focus on *diblock* copolymer architectures as polymer template materials—thus omitting chain connectivity as a relevant parameter for structure formation. This restriction is notable in light of the technological relevance of multiblock copolymer architectures as, for example, thermoplastic elastomers, which also constitute an attractive platform for property engineering by means of particle addition. Diblock copolymers (AB) are unique in that chain ends are symmetrically distributed in both polymer domains, and thus similar structure formation is expected (and observed) for particles that are compatibilized with either the A or B domain. Since chain ends provide additional free volume and relaxation pathways that support the accommodation of particle fillers, different compatibilization characteristics are expected in block copolymers with different chain architecture.

In this contribution we present a systematic study of the implications of block copolymer chain architecture on the compatibility of nanoparticle fillers that are enthalpically neutralized to one of the copolymer domains. Three types of copolymer architecture have been explored in order to understand the effect of chain connectivity and branching on the segregation of particle fillers: linear diblock (AB), triblock (ABA, BAB) and four-arm star (A_3B, AB_3) copolymers. The materials in the present study are based on polyisoprene (PI) and polystyrene (PS) block composition and oligostyrene-functionalized gold nanoparticles (AuPS, core diameter $d_{core} \cong 2.8$ nm, cumulative particle core and shell diameter $d_P \cong 3.8$ nm) as enthalpically neutralized additives to the PS domain. Block copolymer compositions and molecular weights were chosen such as to facilitate lamellar (L) and cylindrical (C) microdomain structures and similar values of the effective particle size parameter $s \cong 0.5$ for all BCP/NP blends. This rather large value of s (previous studies were focused on $s \sim 0.1-0.3$) was chosen based on the expectation that the implications of constraining effects related to chain connectivity increase with particle size (see Discussion section).[5] For all samples the particle concentration was chosen to be $c_P = 1$ wt % (corresponding to a net particle volume filling fraction $\phi_P \cong 0.005$, including the volumes of both particle core and shell) in order to neglect effects related to changes of the overall polymer composition. The different polymer architectures used in the present study are illustrated in Scheme 1.

Our experiments reveal that particle compatibilization depends on the architecture of both the particle-loaded and the particle-free domain. The mutual relevance of the architecture of both domains is interpreted in terms of *direct* and *indirect* constraints that relate to constraining effects due to the connectivity of the particle-loaded domain and to the coupling of dimensional changes that is implied by the covalent linkage between the two blocks. The results thus point to a more complicated parameter space for controlling structure formation in BCP/NP blends that will need to be taken into account if the particle-blending approach is to be applied to copolymer hosts with branched or multiblock architectures.

Scheme 1. Illustration of Chain Architectures of Host Copolymers Used in the Present Study

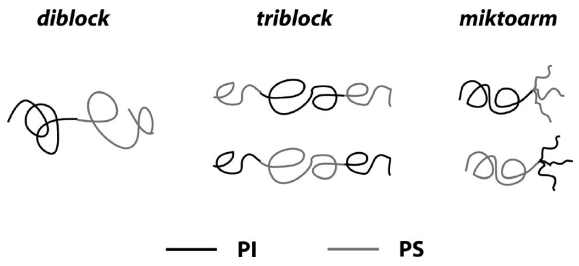

Materials and Methods

Materials. All samples (diblock copolymers of the PS-*b*-PI type and triblock copolymers of the PS-*b*-PI-*b*-PS and PI-*b*-PS-*b*-PI types) were prepared by anionic polymerization using high-vacuum techniques in evacuated, *n*-BuLi-washed, benzene-rinsed glass vessels. The purification of styrene (Acros), isoprene (Acros), and benzene (Lab Scan) to the standards required for anionic polymerization has been described elsewhere.[27] The synthetic procedure used was the sequential addition of monomers and taking into consideration the necessity of high purity of all components. The polymerization reactions of the diblocks as well as the triblocks were controlled by collecting aliquots and conducting size exclusion chromatography (SEC) measurements.

It should be noted that in the case of the PS-*b*-PI-*b*-PS samples the polymerization up to the PS-*b*-PI$^-$Li$^+$ part was accomplished accordingly, but prior to the addition of the second styrenic monomer, a very small amount of polar solvent (THF) was added in order to increase the initiation rate of the styrene toward the PS-*b*-PI$^-$Li$^+$ macroinitiator. The PI-*b*-PS-*b*-PI copolymers were synthesized in a similar way. The only difference was the addition of the polar solvent after the polymerization of the first isoprene quantity in order to increase the initiation and accordingly the propagation rate of the styrene toward the PI$^-$Li$^+$ macroinitiator. Because of the existence of a polar solvent the microstructure of the final synthesized PI chain is altered and became ~54 wt % of 3,4-isomerism, 16 wt % of 1,2-isomerism, and 30 wt % 1,4-isomerism, whereas the initial PI segments exhibit ~90% 1,4-isomerism and the remaining 10% is a combination of mostly 1,2- and 3,4-microstructures.[28,29] Synthesis of the S_3I and SI_3 4-miktoarm star copolymers was performed according to previously published procedures.[30,31] For more information on the quantitative determination of geometric isomerism of the second PI segment of a diblock (PS-*b*-PI type, designated as SI-*L* in Table 1) and a triblock copolymer (PI-*b*-PS-*b*-PI type, designated as ISI-*C* in Table 1), the reader is referred to the Supporting Information (Figure S2 and Table S1) where a detailed analysis of the chemical shifts of all chains is provided.

Where needed, fractionation was carried out by adding methanol to the stirred polymer solution (~0.5% w/v) in toluene at room temperature until turbidity was detected. The mixture was then heated and stirred gently until it became clear, was transferred to a warm separatory funnel and allowed to equilibrate at room temperature overnight. This procedure was repeated until no precursors or undesirable products were shown to be present by size exclusion chromatography (SEC) studies.

Characterization. The molecular characterization was carried out by size exclusion chromatography (SEC), membrane osmometry (MO), and vapor pressure osmometry (VPO). The number-average molecular weights ($\overline{M}_n$) (higher than 15 000 g/mol) of the precursors and the final products were measured with a Gonotec membrane osmometer (MO) Osmomat 090 at 35 °C.

Table 1. Characteristics of the Precursors and the Final Diblock, Triblock, and Miktoarm Star Copolymers Used in the Present Study

sample	$(\overline{M}_n)_{\text{first arm}}$[a] (kg/mol)	$(\overline{M}_w/\overline{M}_n)_{\text{first arm}}$[b]	$(\overline{M}_n)_{\text{total}}$[a] (kg/mol)	$(\overline{M}_w/\overline{M}_n)_{\text{total}}$[b]	$(\phi_{PS})_{\text{copolymer}}$[c]	s[d]
SI-*L*	45.8	1.03	71.5	1.10	0.61	0.57
SIS-*L*	26.0	1.02	93.0	1.05	0.48	0.77
ISI-*L*	24.5	1.05	98.5	1.05	0.46	0.56
I_3S-*L*	41.8	1.02	87.6	1.06	0.48	0.58
IS_3-*L*	43.2	1.02	85.3	1.06	0.45	1.04
SI-*C*	75.8	1.06	94.1	1.09	0.77	0.44
SIS-*C*	42.6	1.02	94.4	1.06	0.76	0.60
ISI-*C*	14.2	1.03	102.5	1.08	0.72	0.45

[a] Membrane osmometry (MO) in toluene at 35 °C. [b] Size exclusion chromatography (SEC) in THF at 35 °C. [c] Volume fraction based on ^{1}H NMR values using the equation $\phi_{PS,copolymer} = f_{PS}\rho_{PI}/(f_{PS}\rho_{PI} + [1 - f_{PS}]\rho_{PS})$ ($\rho_{PS} = 1.06$ g/mL, $\rho_{PI} = 0.93$ g/mL). [d] $s = d_{APuS}/R_{G,PS\text{-block}}$.

Toluene, distilled over CaH_2, was the measuring solvent. The $\overline{M}_n$ values for the MO measurements were determined from the $(\pi/c)^{1/2}$ vs c plots (π is the osmotic pressure and c is the concentration). Square root plots were used in order to minimize the curvature due to the third virial coefficient. More details are given elsewhere.[32,33] In all cases the correlation coefficient was better than 0.99. Number-average molecular weights ($\overline{M}_n$) (lower than 15 000 g/mol) of the precursors were measured with a Gonotec membrane osmometer (MO) Osmomat 070 at 50 °C, which was calibrated with a benzyl solution to determine the consistency of the instrument.

A Thermo Finnigan isocratic pump, a Shodex model RI-101 differential refractometer, and three columns 35 cm in length of the type PLgel 5 μm mixed-C filled with cross-linked PS and porosity range of 10^2-10^6 Å were used for the SEC experiments. THF was the eluent solvent, and all experiments were carried out at 30 °C. Calibration was performed using eight PS standards with variable molecular weights ($\overline{M}_w = 4.3$ kg/mol up to 3100 kg/mol). Prior to calculating the PDIs of the unknown materials, a series of standard PS solutions were tested in order to examine the accuracy of the instrumentation results.

^{1}H NMR determination of the composition of the materials as well as of the geometric isomerism of polyisoprene segments was carried out in $CDCl_3$ at 30 °C using a Varian Unity Plus 300/54 instrument. The molecular characterization results are given in Table 1 for all the samples synthesized.

The synthesis of thiol-terminated oligostyrene ligands (degree of polymerization $N_{PS} \sim 10$) using anionic polymerization as well as the synthesis of oligostyrene-capped gold particles was performed using a modification of the phase-transfer technique developed by Schiffrin and co-workers as described previously.[7,34] The average particle diameter (i.e., the cumulative diameter of particle core and shell) was determined to be $d_P \cong 3.8$ nm. Particle solutions were filtered through membrane filters (0.25 μm pore diameter) prior to use.

Block copolymer−nanoparticle composite films of about 1 mm thickness were obtained by casting a 10% polymer solution in nonpreferential solvent (toluene) mixed with nanoparticles to result in a final amount of inorganic component in the composite of 1 wt %. Solvent was evaporated over a period of 72 h. The resulting films were annealed in a toluene saturated environment for 72 h at 50 °C and subsequently dried in vacuum for 24 h followed by thermal annealing in vacuum for 72 h at 120 °C. For selected samples, longer time thermal annealing conditions (1 week) were chosen in order to verify near-equilibrium conditions.

Films were microsectioned at −120 °C using a LEICA EM FCS cryo-ultramicrotome. To enhance contrast, microsections were stained using osmium tetroxide (obtained from EM Sciences), which selectively stains polyisoprene domains.

Particle size analysis for each BCP/NP composition was performed by analyzing about 1000 particles for at least five different electron micrographs per sample using the NIH ImageJ software that is available for free at http://rsbweb.nih.gov/ij/download.html.

Transmission electron microscopy (TEM) was performed using a JEOL 2000 EX electron microscope operated at 200 kV.

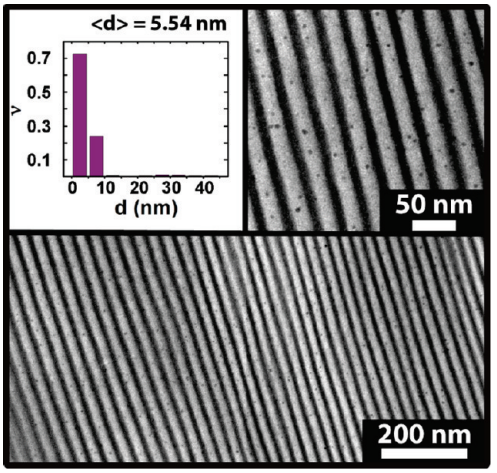

Figure 1. Electron micrograph of the SI-*L*/AuPS composite microstructure (isoprene is dark due to staining with OsO_4). The micrograph reveals that PS-coated gold nanoparticles are mostly single dispersed within PS domain. The left inset depicts the particle size distribution supporting the single particle dispersion (ν denotes the frequency). The average particle diameter is $d_{SI\text{-}L} \cong 5.5$ nm, and the right inset shows a magnified area element.

Imaging was done by amplitude and phase contrast, and images were acquired using a Gatan Orius SC600 high-resolution camera.

Results and Discussion

Table 1 summarizes the characteristics of all material systems used in the present study. The characteristic size ratios, s, were calculated based on the assumption of a cumulative nanoparticle core and shell diameter $d_P = 3.8$ nm and ideal chain configuration of the grafted styrene oligomer as well as the respective PS host domain with $(R_G^2/M_w)^{1/2} = 0.275$ Å mol$^{1/2}$/g$^{1/2}$.[35] The results on linear di- and triblock copolymers will be presented first in order to highlight analogies between BCP/NP blends and block copolymer/homopolymer blends that have been studied extensively in the past. This will provide the context for a qualitative argument to rationalize the effect of branched host copolymer architectures on particle miscibility that will be discussed in the subsequent section.

Linear Di- and Triblock Copolymer Architectures. Figure 1 depicts the cross-sectional electron micrographs for the lamellar SI-*L*/AuPS system revealing that particles are single dispersed within the PS domain, as can be deduced from the average particle diameter that is approximately equal to the neat particle size. A trend is observed for larger particles to segregate within the domain center regions in agreement with previous reports on BCP/NP systems.[15]

ABA-type triblock copolymers differ from the diblock homologues in that the midblock is tethered at both ends and

Scheme 2. Illustration of Bridge (a) and Loop (b) Chain Configurations of the Midblock Domain of Triblock Copolymers in the Microphase-Separated State

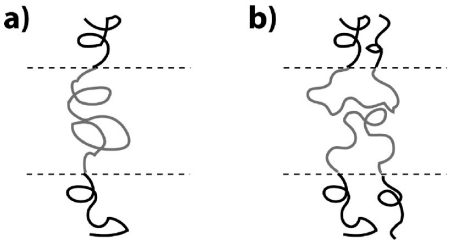

thus—due to the covalent linkage—must assume either looped or bridged conformations in the microphase-separated state, as illustrated in Scheme 2. The formation of "loops" provides a packing environment that is qualitatively similar to diblock copolymers, whereas chain ends are absent for "bridged" chain conformations. Since bridged conformations are expected to occur with ~40% frequency (see Discussion section), a constraining effect is expected for the compatibilization of particle fillers in the midblock domain of triblock copolymers. The effect of chain architecture in linear multiblock copolymers is shown in Figure 2, which depicts electron micrographs of the SIS-*L* and ISI-*L*/AuPS systems. Analysis of the particle size distributions reveals that particles are single dispersed within SIS-*L*, and—analogous to SI-*L*—larger particle sizes are found to preferentially segregate within the center region of PS domains. In contrast, particle aggregation is observed for the ISI-*L*/AuPS system where an average aggregate size of $d_{ISI} \cong 12.1$ nm suggests clustering of about 32 individual nanocrystals (assuming spherical aggregate shape). Note that particles appear to be coagulated within the aggregate structure as deduced by the monolithic aggregate shape. In total, about 90% of the particles can be assigned to aggregate structures in the ISI-*L*/AuPS system. The rather narrow size distribution of aggregates along with their exclusive location within the PS domains suggests that clustering of particles occurs *after* the formation of the copolymer microstructure. In this case, the observed average aggregate size is expected to be a consequence of the spatial constraints on aggregate growth imposed by the adjacent polyisoprene domains, chain packing requirements for accommodation of the particle aggregates, and the dynamics of particles and polymer chains during the annealing process. No significant changes in aggregate size were observed in samples that were annealed for 7 days, suggesting that near-equilibrium conditions have been reached after 3 days of thermal annealing.[36,37]

A comment should be made regarding the relevance of particle coarsening under thermal annealing conditions. Coarsening of organic modified embedded gold nanocrystals at elevated temperatures is a well-known phenomenon and has been attributed to the limited temperature stability of the gold−ligand bond and the resulting partial debonding of ligands during thermal annealing.[38] The effect of coarsening on the average particle dimensions can be estimated, for example, in the compatible blend system SIS-*L*/AuPS that reveals an increase of the average particle size to $d_{core,72\,h} \cong 5$ nm after 72 h of thermal annealing. A similar coarsening kinetics was observed in homopolymer matrices (see Supporting Information). If the coarsening kinetics is assumed to be approximately independent of the polymer architecture, then both processes—coarsening and aggregation—can be distinguished based on the significantly different dimensional changes associated with each process.

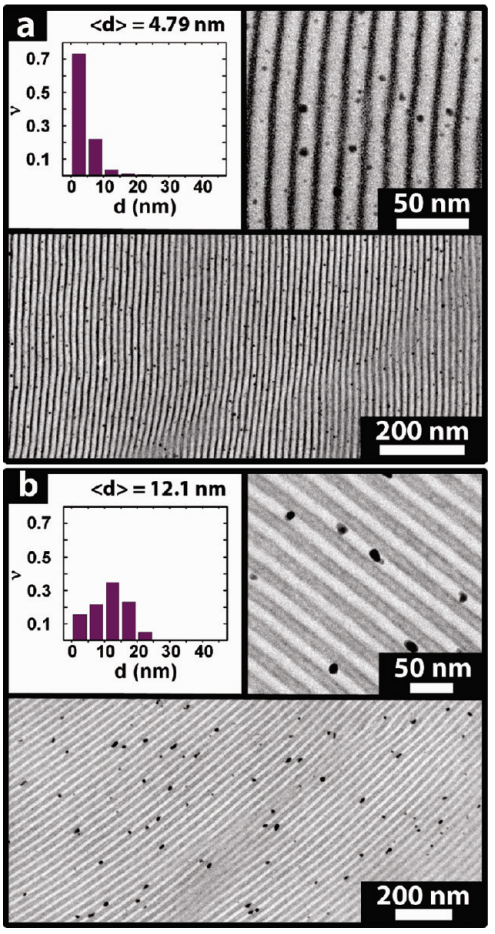

Figure 2. Electron micrographs of triblock copolymer/particle blend systems revealing particle aggregation in the triblock mid-domain (isoprene is dark due to staining with OsO_4). Panel a: SIS-*L*/AuPS composite microstructure revealing single particle dispersion (average particle diameter $d_{SIS\text{-}L} \cong 4.8$ nm). Panel b: ISI-*L*/AuPS microstructure revealing the formation of approximately equal sized aggregates ($d_{ISI\text{-}L} \cong 12.1$ nm). About 90% of particles are part of aggregates. In both panels the left inset depicts the particle size distribution (ν denotes the frequency), and the right inset shows a magnified area element.

This is the fundamental assumption underlying our interpretation.

Figure 3 confirms the similar structure formation characteristics of the linear cylindrical BCP/NP systems (with PS being the majority domain) as compared to the lamellar analogues. Particle size distributions reveal approximately single particle dispersions for SI-*C* and SIS-*C* host copolymers and particle aggregation for the ISI-*C*/AuPS system. In the latter case, an average aggregate size of $d_{ISI} \cong 16.1$ nm suggests clustering of about 76 individual nanocrystals per aggregate. Note that in the case of the ISI-*C*/AuPS system aggregation is observed despite a value of s that is only about half compared to the lamellar SIS system ($s_{ISI\text{-}C} \cong 0.5 s_{SIS\text{-}L}$), thus underscoring the constraining effect on particle segregation that is associated with the connectivity of the midblock polymer domain.

The observed architecture effect on particle segregation displays interesting analogies to the related system of block copolymer/homopolymer (BCP/hP) blends. For example, hP additives with molecular weight less than the respective copolymer host block have been found to be miscible with both diblock and triblock end-domains (also, in these studies the maximum hP solubility was found to increase with decreasing hP molecular weight).[39−41] In contrast,

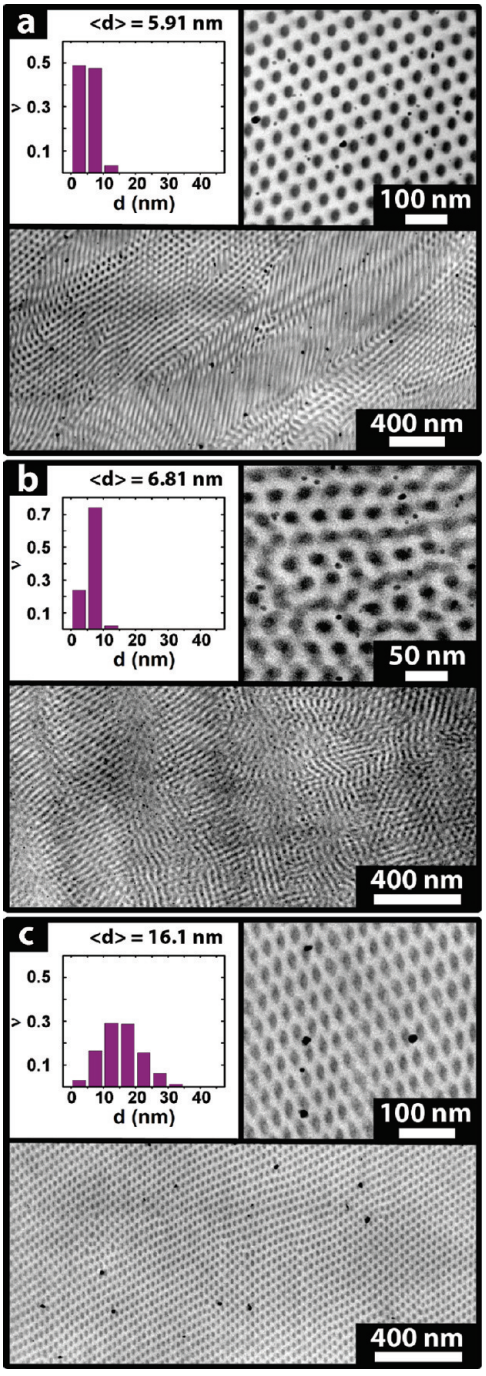

Figure 3. Electron micrographs of the SI-*C*/AuPS (panel a), SIS-*C*/AuPS (panel b), and ISI-*C*/AuPS (panel c) systems (isoprene is dark due to staining with OsO_4). The micrographs reveal single particle dispersion in the case of diblock or end block connectivity of the polystyrene host domain (SI-*C*, $d_{SI\text{-}C} \cong 5.9$ nm; SIS-*C*, $d_{SIS\text{-}C} \cong 6.8$ nm) and aggregate formation for the midblock connected polystyrene host domain (ISI-*C*, $d_{ISI\text{-}C} \cong 16.1$ nm). In SI-*C*, partial aggregation of particles is observed along the grain boundary regions which results in an overestimate of the average particle size. In all panels the left inset depicts the particle size distribution (ν denotes the frequency), and the right inset shows a magnified area element.

reduced solubility as well as heterogeneous distribution within the domain microstructure was reported when hP was dispersed in triblock mid-domains.[42−44] We interpret the reduced particle miscibility in triblock mid-domains to be a consequence of the entropy loss associated with the uniformly stretched conformation of bridged midblock chains that was (to our knowledge) first postulated by Semenov.[45] More recent self-consistent field simulations have shown for symmetric triblock copolymers with $\chi N \sim 30$ (χ denotes the Flory interaction parameter, N is the degree of polymerization) that the probability of forming bridged conformations is in the range of 40%—similar estimates were concluded from experimental studies by Watanabe.[46−48] We hypothesize that the significant fraction of bridged chains impedes particle sequestration. While there is currently no reference to quantitatively relate the availability of chain ends to particle miscibility, recent theoretical studies on the penetration of particle fillers in polymer brushes by Kim and O'Shaughnessy provide an instructive analogy in support of this argument. On the basis of a SCF theoretical analysis of brush/nanoparticle systems, the authors concluded that the "softening" of a polymer brush in the vicinity of its surface due to chain-end relaxation is responsible for the segregation of particle fillers (with diameter larger than the polymer thermal blob size) to the brush surface.[49,50]

In order to provide a qualitative rationale for the dependence of particle compatibility on the constitution of both the particle-loaded and the particle-free domains, it is helpful to consider the dimensional changes of block copolymer domains associated with the addition of filler particles. Because of the covalent linkage, adjacent blocks must retain an equal interfacial area per junction, σ, if the lamellar microstructure is to be maintained. The resulting coupling of dimensional changes of the respective block domains render the mixing process dependent on the architecture of *all* constituting blocks. For layered BCP/NP systems with uniform particle distribution (within the compatible block), the change in domain dimensions can be estimated using a free energy argument first postulated by Ausserré and coworkers.[9] For example, for a lamellar diblock copolymer with volume fraction $f = N_A/(N_A+N_B)$ of the particle-filled (A) domain (N_i is the degree of polymerization of the ith block), the dependence of the layer dimension on the particle volume filling fraction ϕ_P can written as (see Supporting Information)

$$L_{P,0}/L_0 = \Lambda^{-1/3}(f,\phi_P)\frac{1}{1-\phi_P} \quad (1a)$$

$$l^A_{P,0}/l^A_0 = \Lambda^{-1/3}(f,\phi_P)\left(1+\frac{1}{f}\frac{\phi_P}{1-\phi_P}\right) \quad (1b)$$

$$l^B_{P,0}/l^B_0 = \Lambda^{-1/3}(f,\phi_P) \quad (1c)$$

where $\Lambda(f,\phi_P) = (f + (1-f)\phi_P{}^2)/(f(1-\phi_P)^2)$, $L_{P,0}$ and L_0 denote the equilibrium lamellar spacing, and $l^i_{P,0}$ and l^i_0 are the segment length of the ith block in the particle-filled and neat block copolymer, respectively, as illustrated in Scheme 3.[51] Note that for symmetric polymer compositions ($f = 0.5$) and including only first-order terms in ϕ_P eqs 1a−1c reduce to Ausserré's result, i.e., $L_{P,0} = L_0(1+\phi_P/3)$, $l^A_{P,0} = l^A_0(1+4\phi_P/3)$ and $l^B_{P,0} = l^B_0(1-2\phi_P/3)$. The change of the interfacial area per junction upon particle addition can be determined from eqs 1a−1c as $\sigma_{P,0} = 2Nb^3/L_{P,0} = \sigma_0\Lambda^{1/3}(f,\phi_P) \cong \sigma_0(1+2\phi_P/3)$, where $\sigma_0 = 2Nb^3/L_0$ denotes the equilibrium interfacial area per junction of the neat block copolymer, N is the total degree of polymerization, and b is the (average) monomer size. Thus, the block-selective dispersion of particle fillers within a BCP is expected to induce axial and lateral swelling of the particle-filled polymer domain. Because of the constraint of equal interfacial area per junction, the lateral swelling induces axial compression of the particle-free polymer domains. This mutual dependence of structural changes upon particle addition is a

Scheme 3. Illustration of the Coupling of Dimensional Changes in Block Copolymer Domains Induced by the Addition of Filler Particles[a]

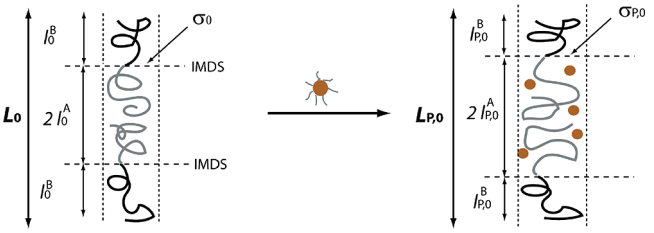

[a] The increase of interfacial area per junction results in compression of the particle-free domain (IMDS denotes the intermaterial dividing surface). See text for more details.

consequence of the constraint of equal interfacial area per junction of the covalently connected blocks and will be of relevance for rationalizing the compatibility of particle fillers in star copolymers that will be discussed in the next section.

We note that because of the dominant scattering of the high electron density gold particle cores and the small particle volume filling fraction, it has not been possible to validate eqs 1a−1c for the present material systems. However, the predicted change in layer dimensions qualitatively agrees with previous reports on the effect of low-molecular-weight hP additives on the layer dimensions of diblock copolymer host materials that have been studied over a wide compositional range.[39] Since the assumption underlying eqs 1a−1c is the uniform distribution of particle inclusions, the predictions are independent of the nature of the additive and thus applicable to a wide range of blend constituents.

Miktoarm Star Copolymer Architectures. Star copolymer architectures differ from their linear homologues in both constitutional and conformational asymmetry that results in a shift of the morphological stability regions as compared to linear block copolymers.[52−54] In the limit of strongly segregated star copolymers, Milner proposed the structure formation to depend on the chain architecture parameter $\varepsilon = (n_A/n_B)(p_A/p_B)^{1/2}$ with n_i denoting the number of arms of component "i", $p_i = M/(\rho\langle R^2\rangle_0 N_{Av})$ is the chain packing density, and M, ρ, $\langle R^2\rangle_0$, and N_{Av} represent the molecular weight, density, average square end-to-end distance, and Avogadro's number, respectively.[52] Using both Milner's mean-field theory and experimental studies, Floudas and co-workers demonstrated that the maximum effect of chain branching on the segregation strength of star copolymers is attained for four-arm architectures of type AB_3.[55] Based on this assertion, the effect of chain architecture on particle segregation was tested for compositionally symmetric SI_3-L and S_3I-L systems with total degree of polymerization approximately equal to the linear block copolymer homologues (see Table 1). Since $p_{PI}/p_{PS} \cong 0.84$ at $T = 25$ °C, it follows that $\varepsilon_{SI_3\text{-}L} \cong 2.75$ and $\varepsilon_{S_3I\text{-}L} \cong 3.27$, and thus, both polymer systems are expected to exhibit similar segregation conditions.

Figure 4 depicts electron micrographs of the SI_3-L/AuPS and S_3I-L/AuPS systems, revealing particle aggregation in both miktoarm samples irrespective of the architecture of the particle-bearing polymer domain. The average diameter of particle aggregates is found to be similar (and about equal to the PS-layer thickness); i.e., $d_{SI_3\text{-}L} \cong d_{S_3I\text{-}L} \cong 18$ nm, suggesting the clustering of about 106 nanocrystals per aggregate. We rationalize the reduced compatibility of particle fillers within the S_3I-L/AuPS system to be a consequence of the large effective particle size $s \cong 1$ that implies a significant

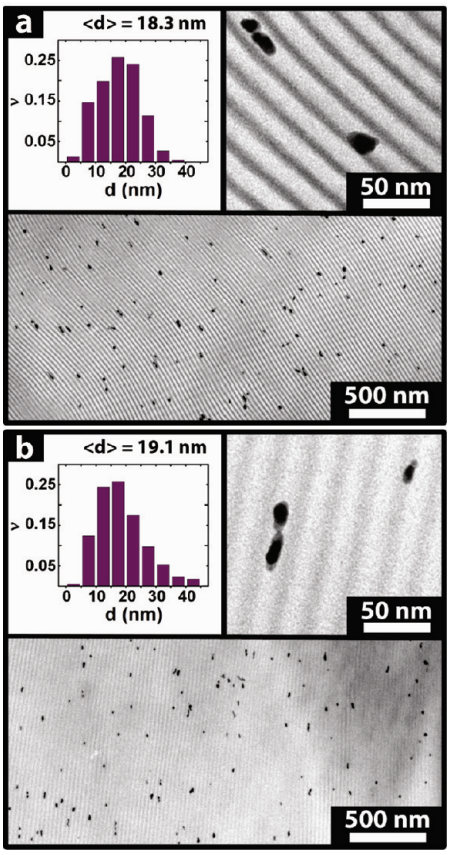

Figure 4. Electron micrographs of the SI_3-L/AuPS (panel a) and S_3I-L/AuPS (panel b) systems (isoprene is dark due to staining with OsO_4). In both cases particle aggregation is observed with approximately equal aggregate size where $d_{SI_3\text{-}L} = 18.3$ nm and $d_{S_3I\text{-}L} = 19.1$ nm (corresponding to 111 and 126 nanocrystals per aggregate), respectively. In both panels the left inset depicts the particle size distribution (ν denotes the frequency), and the right inset shows a magnified area element.

penalty in conformational entropy if particles are to be accommodated by the polymer chains. This effect is expected to be more pronounced in star polymer systems where segmental crowding in the vicinity of the interface results in stretching of the polymer chains.

In contrast to the S_3I-L/AuPS system, the aggregation of particle fillers within the SI_3-L host polymer is notable because the characteristic ratio of the styrene domain is approximately equal to the SI-L system with $s \cong 0.57$. We interpret the reduced particle compatibility as a consequence of the segmental crowding in the adjacent PI miktoarm domain which is required to compress upon swelling of the linear particle-loaded block domain (this is true assuming that particles do not exclusively segregate along the PS-domain center region). Since, as discussed earlier, an equal interfacial area per junction has to be maintained for both block domains, lateral expansion of the PS domain will result in axial compression of the adjacent star polymer domain. Because of the smaller equilibrium end-to-end distance of the branched blocks, as well as the segmental crowding and associated chain stretching, the compression of the star copolymer domain will necessarily involve a higher energy penalty compared to the corresponding diblock copolymer system, thus impeding particle sequestration.

We note that the reported effect of chain architecture on the compatibility of particle fillers was found to be sensitive to the mechanism of annealing, i.e., thermal or solvent

annealing. In particular, aggregate formation in the SI_3-*L*/AuPS system was only observed after thermal annealing (see Figure S4). We hypothesize that structures formed by solvent annealing (even in case of neutral solvents) do not represent thermal equilibrium conditions due to screening and kinetic trapping effects. A similar argument was made recently by Matsen et al. (see ref 25). This aspect should be taken into account when comparing experimentally observed microstructures with those observed in simulation studies.

Conclusion

The compatibility of enthalpically neutralized particle fillers with effective size $s \cong 0.5$ has been found to sensibly depend on the architecture of block copolymer host materials. For linear triblock copolymers, the connectivity of the midblock domain extends a *direct* constraint impeding particle sequestration that has been interpreted as a consequence of the entropy loss associated with the accommodation of particle fillers due to the stretched configuration of bridged midblock chains. For four-arm star copolymers, both *direct* and *indirect* constraints associated with the characteristic dimension, *s*, and the mutual dependence of conformational changes due to the covalent linkage are proposed as rationale for the observed particle aggregation. Since our interpretation rests on the effect of particle fillers to restrict chain conformations, the expectation is that the implications of both constraints in systems with equal particle number density will be alleviated with decreasing particle size (i.e., decreasing characteristic ratio *s*) and increasingly favorable enthalpic interactions. In summary, our results point to a more complicated parameter space for controlling structure formation in BCP/NP blend systems that will need to be taken into account if the particle-blending approach is to be applied to branched or multiblock copolymer architectures.

Acknowledgment. Financial support by the National Science Foundation via Grant DMR0706265 and the MRSEC program of the National Science Foundation under Award DMR-0520425 as well as by the Greek Secretariat for Research & Development through the bilateral project 05-NONEU-229 handled by the Research Committee, University of Ioannina (A.A.) is gratefully acknowledged.

Supporting Information Available: Electron micrographs of neat AuPS; electron micrographs of hPS/AuPS after 3 days of thermal annealing; ^{1}H NMR characterization of constitutional isomerism; electron micrograph of solvent-annealed microstructures; derivation of eqs 1a−1c. This material is available free of charge via the Internet at http://pubs.acs.org.

References and Notes

(1) *Chemical Industry R&D Roadmap for Nanomaterials by Design*, Chemical Industry Vision2020 Technology Partnership, 2003.
(2) Whitesides, G. M.; Grzybowski, B. *Science* **2002**, *295*, 2418.
(3) Park, C.; Yoon, J.; Thomas, E. L. *Polymer* **2003**, *44*, 6725.
(4) Balazs, A. C.; Emrick, T.; Russell, T. P. *Science* **2006**, *314*, 1107.
(5) Bockstaller, M. R.; Mickiewicz, R.; Thomas, E. L. *Adv. Mater.* **2005**, *17*, 1331.
(6) Warren, S. C.; Messina, L. C.; Slaughter, L. S.; Kamperman, M.; Zhou, Q.; Gruner, S. M.; DiSalvo, F. J.; Wiesner, U. *Science* **2008**, *320*, 1748.
(7) Bockstaller, M. R.; Kolb, R.; Thomas, E. L. *Adv. Mater.* **2001**, *13*, 1783.
(8) Bockstaller, M. R.; Thomas, E. L. *Phys. Rev. Lett.* **2004**, *93*, 166106.
(9) Hamdoun, B.; Ausserre, D.; Joly, S.; Gallot, Y.; Cabuil, V.; Clinard, C. *J. Phys. II* **1996**, *6*, 493.
(10) Hamdoun, B.; Ausserre, D.; Cabuil, V.; Joly, S. *J. Phys. II* **1996**, *6*, 503.
(11) Lauter-Pasyuk, V.; Lauter, H. J.; Ausserre, D.; Gallot, Y.; Cabuil, V.; Kornilov, E. I.; Hamdoun, B. *Phys. B* **1997**, *241*, 1092.
(12) Lee, J. Y.; Thompson, R. B.; Jasnow, D.; Balazs, A. C. *Phys. Rev. Lett.* **2002**, *89*, 155503.
(13) Thompson, R. B.; Ginzburg, V. V.; Matsen, M. W.; Balazs, A. C. *Macromolecules* **2002**, *35*, 1060.
(14) Thompson, R. B.; Ginzburg, V. V.; Matsen, M. W.; Balazs, A. C. *Science* **2001**, *292*, 2469.
(15) Bockstaller, M. R.; Lapetnikov, Y.; Margel, S.; Thomas, E. L. *J. Am. Chem. Soc.* **2003**, *125*, 5276.
(16) Kim, B. J.; Bang, J.; Hawker, C. J.; Kramer, E. J. *Macromolecules* **2006**, *39*, 4108.
(17) Chiu, J. J.; Kim, B. J.; Kramer, E. J.; Pine, D. J. *J. Am. Chem. Soc.* **2005**, *127*, 5036.
(18) Kim, B. J.; Chiu, J. J.; Yi, G. R.; Pine, D. J.; Kramer, E. J. *Adv. Mater.* **2005**, *17*, 2618.
(19) Lo, C.-T.; Lee, B.; Pol, V. G.; Dietz Rago, N. L.; Seifert, S.; Winans, R. E.; Thiyagarajan, P. *Macromolecules* **2007**, *40*, 8302.
(20) Gaines, M. K.; Smith, S. D.; Samseth, J.; Bockstaller, M. R.; Thompson, R. B.; Rasmussen, K. Ø.; Spontak, R. J. *Soft Matter* **2008**, *4*, 1609.
(21) Spontak, R. J.; Shankar, R.; Bowman, M. K.; Krishnan, A. S.; Hamersky, M. W.; Samseth, J.; Bockstaller, M. R.; Rasmussen, K. Ø. *Nano Lett.* **2006**, *6*, 2115.
(22) Listak, J.; Bockstaller, M. R. *Macromolecules* **2006**, *39*, 5820.
(23) Pryamitsyn, V.; Ganesan, V. *Macromolecules* **2006**, *39*, 8499.
(24) Sides, S. W.; Kim, B. J.; Kramer, E. J.; Fredrickson, G. H. *Phys. Rev. Lett.* **2006**, *96*, 250601.
(25) Matsen, M. W.; Thompson, R. B. *Macromolecules* **2008**, *41*, 1853.
(26) Reis, F. D. A. *Macromolecules* **2008**, *41*, 8932.
(27) (a) Hadjichristidis, N.; Iatrou, H.; Pispas, S.; Pitsikalis, M. *J. Polym. Sci., Part A: Polym. Chem.* **2000**, *38*, 3211. (b) Iatrou, H.; Avgeropoulos, A.; Hadjichristidis, N. *Macromolecules* **1994**, *27*, 6232.
(28) Avgeropoulos, A.; Paraskeva, S.; Hadjichristidis, N.; Thomas, E. L. *Macromolecules* **2002**, *35*, 4030.
(29) (a) Rangou, S.; Avgeropoulos, A. *J. Polym. Sci., Part A: Polym. Chem.* **2009**, *47*, 1567. (b) Avgeropoulos, A.; Rangou, S.; Krikorian, V.; Thomas, E. L. *Macromol. Symp.* **2008**, *267*, 16.
(30) Iatrou, H.; Siakali-Kioulafa, E.; Hadjichristidis, N.; Roovers, J.; Mays, J. W. *J. Polym. Sci., Part B: Polym. Phys.* **1995**, *33*, 1925.
(31) Avgeropoulos, A.; Hadjichristidis, N. *J. Polym. Sci., Part A: Polym. Chem.* **1997**, *35*, 813.
(32) Iatrou, H.; Hadjichristidis, N. *Macromolecules* **1992**, *25*, 4649.
(33) Iatrou, H.; Hadjichristidis, N. *Macromolecules* **1993**, *26*, 2479.
(34) Brust, M.; Walker, M.; Bethell, D.; Schiffrin, D. J.; Whyman, R. *J. Chem. Soc., Chem. Commun.* **1994**, 801.
(35) Cotton, J. P.; Decker, D.; Benoit, H.; Farnoux, B.; Higgins, J.; Jannink, G.; Ober, R.; Picot, C.; desCloizeaux, J. *Macromolecules* **1974**, *7*, 863.
(36) This is in agreement with the observation that 90% of filler particles are clustered after 3 days of thermal annealing.
(37) Three days of thermal annealing was chosen as a reference state in our studies since debonding of ligands by thermally activated cleavage of gold−thiol bonds renders long-time annealing results ambiguous. Reference studies on blends of AuPS in homopolystyrene indicated some coarsening after 3 days of thermal annealing; however, the associated change in particle dimensions was found to be small compared to the observed aggregate dimensions (see Supporting Information, Figure S3).
(38) Meli, L.; Green, P. F. *ACS Nano* **2008**, *2*, 1305.
(39) Winey, K. I.; Thomas, E. L.; Fetters, L. J. *Macromolecules* **1991**, *24*, 6182.
(40) Tanaka, H.; Hasegawa, H.; Hashimoto, T. *Macromolecules* **1991**, *24*, 240.
(41) Hashimoto, T.; Tanaka, H.; Hasegawa, H. *Macromolecules* **1990**, *23*, 4378.
(42) Lee, S.-H.; Koberstein, J. T.; Quan, X.; Gancarz, I.; Wignall, G. D.; Wilson, F. C. *Macromolecules* **1994**, *27*, 3199.
(43) Baetzold, J. P.; Gancarz, I.; Quan, X.; Koberstein, J. T. *Macromolecules* **1994**, *27*, 5329.
(44) Jiang, M.; Cao, X.; Yu, T. *Polymer* **1986**, *27*, 1923.
(45) Semenov, A. N. *Sov. Phys. JETP* **1985**, *61*, 733.
(46) Matsen, M. W.; Thompson, R. B. *J. Chem. Phys.* **1999**, *111*, 7139.
(47) Jones, R. L.; Kane, L.; Spontak, R. J. *Chem. Eng. Sci.* **1996**, *51*, 1365.
(48) Watanabe, H. *Macromolecules* **1995**, *28*, 5006.

(49) Kim, J. U.; O'Shaughnessy, B. *Phys. Rev. Lett*. **2002**, *89*, 238301.
(50) Kim, J. U.; O'Shaughnessy, B. *Macromolecules* **2006**, *39*, 413.
(51) In the derivation of eqs 1a−1c, equal size of the repeat units of both polymer constituents has been assumed (see Supporting Information).
(52) Milner, S. T. *Macromolecules* **1994**, *27*, 2333.
(53) Tselikas, Y.; Iatrou, H.; Hadjichristidis, N.; Liang, K. S.; Mohanty, K.; Lohse, D. J. *J. Chem. Phys*. **1996**, *105*, 2456.
(54) Yang, L.; Hong, S.; Gido, S. P.; Velis, G.; Hadjichristidis, N. *Macromolecules* **2001**, *34*, 9069.
(55) Floudas, G.; Hadjichristidis, N.; Tselikas, Y.; Erukhimovich, I. *Macromolecules* **1997**, *30*, 3090.